Renewable Energy 77 (2015) 159–165

Contents lists available at ScienceDirect

Renewable Energy

journal homepage: www.elsevier.com/locate/renene

Deformation and instability failure of borehole at high temperature and high pressure in Hot Dry Rock exploitation

Yangsheng Zhao [a, *], Zijun Feng [a], Baoping Xi [a], Zhijun Wan [b], Dong Yang [a], Weiguo Liang [a]

[a] College of Mining Technology, Taiyuan University of Technology, Taiyuan, Shanxi 030024, China
[b] School of Mines, China University of Mining & Technology, Xuzhou, Jiangsu 221116, China

ARTICLE INFO

Article history:
Received 6 February 2014
Accepted 26 November 2014
Available online 23 December 2014

Keywords:
Granite
High temperature and high pressure
Creep
Borehole stability
Ultimate drilling depth

ABSTRACT

Borehole stability at high temperature and high in-situ stresses is the key to Hot Dry Rock geothermal energy extraction. Upon drilling completion, borehole stability, its deformation and failure critical condition will be significant in deep HDR engineering design and construction. Using high temperature and high pressure servo-controlled triaxial rock testing machine, we performed experiments of borehole deformation and instability for three granite samples (200 mm in diameter and 400 mm long with a 40 mm opening in the center) at different hydrostatic stresses and temperature. The elastic and creep deformation data was analyzed. The results indicate that: 1) when the hydrostatic pressure is lower than 100 MPa and the temperature is below 400 °C, the specimens deform following the generalized Kelvin model. The critical condition for borehole stability is reached at hydrostatic pressure of 125 MPa and temperature of 500 °C, when creep deformation accelerates sharply. The failure mode is shear failure or a combination of shear and tension failure. The critical radial deformation ratio is about 20%; 2) Creep deformation at steady creep phase is derived based on the test data. The ultimate condition for drilling in granite is analyzed in regards to temperature and in-situ stresses.

1. Introduction

Hot Dry Rock (HDR) geothermal energy is mainly stored in granite. To exploit HDR geothermal energy, we need a great amount of drilling in granite, especially deep boreholes that are used to form artificial reservoir mainly through hydraulic fracturing technologies [1–3]. For other applications such as searching oil and gas resources, a lot of super-deep borings are located in the high temperature and high stress rock. Such projects have been carried out as Continental Scientific Drilling in more than ten countries, such as Russia, Germany, United States, and China. In Russia, the Kola SG-3 ultra-deep drilling at Kola Peninsula is 12262 m deep [4]. KTB-HB ultra-deep drilling in Germany is 9101 m deep [5]. Chinese continental scientific drilling conducted from June 2001 to January 2005 is 5118.2 m [6]. The first drilling for extracting hot dry rock geothermal energy at Fenton hill site in New Mexico is 4400 m [7,8]. Successful deep drilling under high temperature and high stresses is the key to explore energy and resources of the deep crust. At room temperature, the development of intra-and trans-granular dilatant microcracks in crystalline granite leads to borehole instability in the form of breakouts [9]. However, the physical and mechanical properties in rocks will change with temperature such as elastic modulus reduction [10], permeability enhancement [11], and mechanical strength decrease [12]. As a consequence, problems arise related to the borehole deformation and stability under high temperature and high stress, under which conditions, rock mass may lose its strength and exhibit rheological behavior [13].

Because of temperature and stress corrosion effects at depth [14], the drilling and completing cost is higher than that in oil and gas industry [15,16]. And the necking deformation, instability, and collapsing of boreholes in drilling always lead to a substantial increase in drilling costs and the borehole maintenance costs, and even sometimes prevent the project to be implemented [17]. Hence, in-depth study of borehole deformation and instability critical conditions under high temperature and high stress is of great scientific and engineering significance.

In this paper, the authors present the test results of granite rock specimens using the 20 MN servo-controlled high temperature and high pressure triaxial rock testing machine [18]. Three specimens were tested under less than 600 °C and 150 MPa hydrostatic stress. The deformation of the granite specimens, including elastic and

* Corresponding author. Tel./fax: +86 0351 6014865.
E-mail address: y-s-zhao@263.net (Y. Zhao).

http://dx.doi.org/10.1016/j.renene.2014.11.086
0960-1481/

creep deformation, was recorded and analyzed under steady and critical conditions for instability destroy of borehole.

2. Rock specimen testing under high hydrostatic pressure and high temperature

2.1. Experimental setup and monitoring equipment

The experimental setup shown in Fig. 1 has the following parameters:

1) Maximum axial load: 10,000 kN;
2) Maximum lateral load: 10,000 kN;
3) Maximum axial pressure on rock specimen: 318 MPa;
4) Maximum lateral pressure on rock specimen: 250 MPa (pseudo-triaxial confining pressure);
5) Maximum pore pressure: 250 MPa;
6) Specimen size: 200 mm × 400 mm;
7) Maximum drilling displacement: 450 mm;
8) Maximum drilling loading: 200 kN;
9) Maximum torque: 500 N m;
10) Maximum heating temperature: 600 °C;
11) Holding time of pressures: over 360 h;
12) Axial and lateral pressure offset: less than 0.3%;

The stress, deformation, pore pressure of inlet and outlet, temperature, torque and other parameters can be automatically recorded. The stiffness of the whole machine is greater than 9×10^{10} N/m.

The deformation of rock specimen and the borehole radial is measured using high temperature displacement sensor combined with static resistance strain gauge while temperature is under 240 °C. But the sensor cannot measure the displacement at the temperature over 240 °C for the serious changes of resistance with high temperature. So a specially designed optical instrument is used to measure borehole deformation during testing under high temperatures (seen in Fig. 2). Acoustic Emission (AE) is also monitored and recorded during the testing.

2.2. Specimen preparation

The granite used in the testing came from Pinyi, Shandong province in China. It is also called “Luhui” granite due to its characteristic of grey color. The samples were taken 50 m deep from a project site and contained no fractures. The three specimens were prepared as cylinders of 200 mm in diameter and 400 mm long. The specimens were cut smoothly on all sides. A hole of 40 mm in diameter was drilled

Fig. 1. 20 MN servo-controlled triaxial rock testing machine.

Fig. 2. Optical borehole deformation observation instrument.

along the cylinder axis of each specimen to simulate a borehole. The prepared specimen is shown in Fig. 3. Drilling of the holes was carefully controlled to ensure their verticality and concentricity. There were no apparent damages or fractures on any of the prepared specimens. The average uniaxial compressive strength (UCS), tensile strength, elastic modulus, and poisson's ratio of samples is 130 MPa, 18 MPa, 35 GPa, 0.25, respectively at normal temperature. The mineral composition is illite (25%), quartz (28%), feldspar (43%), calcite (1%), siderite (1%) and others (2%), respectively. The percentages in the bracket represent quality.

2.3. Testing procedure

The testing procedures are summarized as following:

1) Measure specimen height, diameter and the hole diameter.
2) Install a metal measuring rod in the middle point of the hole. Also install lighting at the bottom of the hole.
3) Seal the specimen and start testing by increasing temperature and hydrostatic pressure to the pre-determined values. The increment is 3–5 °C per hour for temperature.
4) At each pre-determined temperature (200, 300, …, 600), maintain the temperature and all-around pressure and continuously record the axial and radial deformation of the specimen as well as loading and temperature.
5) Measure borehole deformation every hour using the optical borehole deformation observation instrument.

2.4. Testing results of specimen 2

It is expected that the HDR geothermal energy resource exploration and other deep underground projects involve the high

Fig. 3. Granite specimen.

Table 1
Experimental schedule and deformation characteristics of specimen 2.

Duration/hour	Temperature/°C	Hydrostatic pressure/MPa	Deformation of borehole	Axial deformation
0–20	RT-200 °C	12.5	Steady creep	Steady creep
20–38		25	Steady creep	Steady creep
28–77	*200 °C	25	Steady creep	Steady creep
77–125		50	Steady creep	Steady creep
133–178	*250 °C	50	Steady creep	Steady creep
188–230	*300 °C	75	Steady creep	Steady creep
250–275	*400 °C	100	Steady creep	Steady creep
275–290	400–500 °C	125		Less thermal expansion effect, weakening plays a dominant role
290–330	*500 °C	125	Steady creep-accelerated creep-failure	

RT denotes room temperature; the sign* denotes constant temperature.

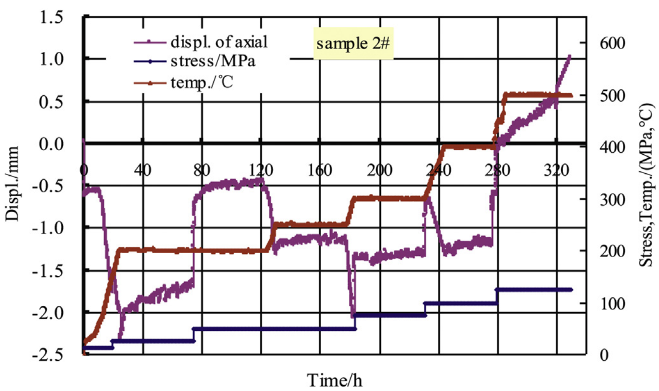

Fig. 4. Total axial displacement due to thermal and stress vs. time of sample 2.

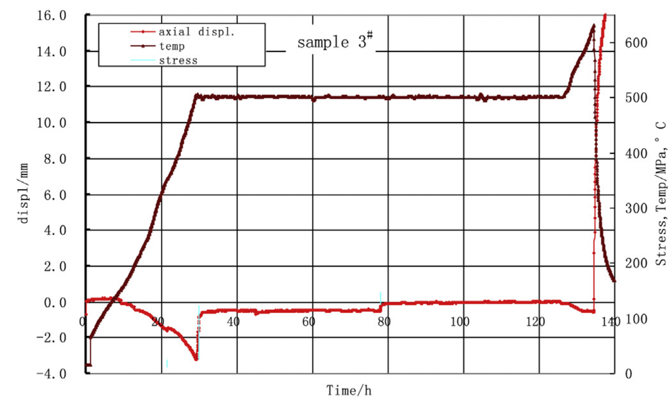

Fig. 6. Total axial deformation due to thermal and stress vs. time of sample 3.

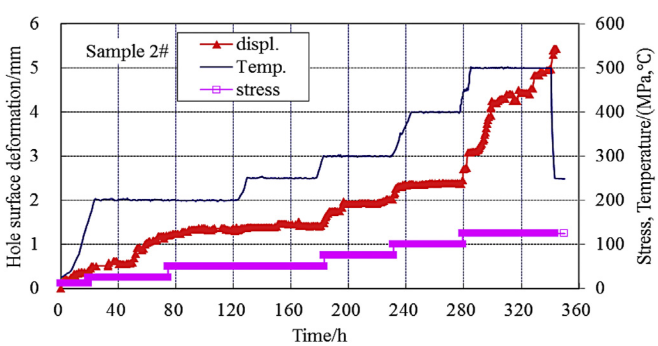

Fig. 5. Borehole deformation due to thermal and stress vs. time of sample 2.

temperature and high stress properties of rock mass. In addition, the in-situ stresses state in deep rock mass are close to hydrostatic [19]. The testing presented herein is designed to be under hydrostatic pressures. Given rock mass unit weight of approximate 2.5 g/cm^3, the vertical stress in 1000 m deep rock mass is close to 25 MPa. The maximum hydrostatic stress applied to the experimental samples is 150 MPa and the maximum temperature is 600 °C. This is comparable to the rock mass of 6000 m deep.

The testing schedule and parameters for specimen 2 are listed in Table 1. The test was run for 330 h Figs. 4 and 5 show the axial deformation and borehole radial deformation of specimen 2, respectively. The axial deformation exhibits steady creep at 400 °C and hydrostatic stress of 100 MPa. It not only decreases due to expansion with increasing temperature but also increases with increasing hydrostatic pressure. When the temperature increased from 400 °C to 500 °C and the hydrostatic pressure increased from 100 MPa to 125 MPa, the axial deformation accelerated. With consistent 500 °C and 125 MPa hydrostatic pressure, the specimen deforms with a high speed, a sign indicates that the rock is close to failure or in its critical condition.

The radial deformation of borehole follows a similar path shown in Fig. 5. It exhibits steady creep at 400 °C and hydrostatic pressure

Table 2
Experiment schedule and deformation characteristics of specimen 3.

Duration/hour	Temperature/°C	Hydrostatic pressure/MPa	Borehole deformation	Axial deformation
0–21	RT to 500 °C	12.5	Steady creep	Steady creep
21–30		25	Steady creep	Steady creep
30–78	*500 °C	125	Steady creep	Steady creep
78–125	*500 °C	150	Steady creep, accelerate creep starting	Steady creep, accelerate creeping starting
125–135	500–600 °C	150	Accelerated creep to failure	

RT denotes room temperature; the sign* denotes constant temperature.

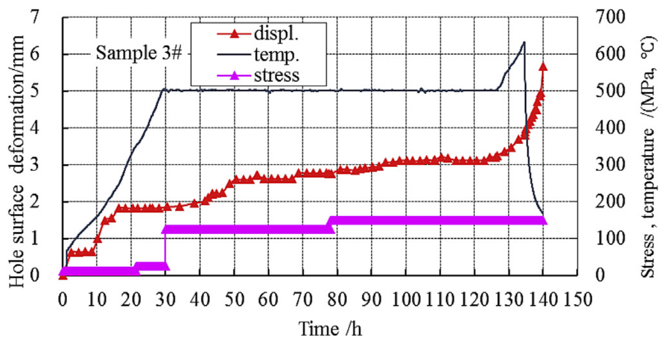

Fig. 7. Borehole deformation due to thermal and stress vs. time of specimens 3.

Table 3
Measured axial creep deformation of specimen 1.

Stress/MPa	Temperature/°C	Single state creep	Creep time/hour	Accumulating creep
12.5	100	0.025	36.667	0.025
25	200	0.14	45.237	0.165
75	300	0.235	42.9	0.4
100	400	0.112863	44.233	0.512863
125	400	0.125	43.833	0.637863
125	500	0.07	34.13	0.707863

of 100 MPa and accelerated creep when temperature increases from 400 °C to 500 °C and the hydrostatic pressure increases to 125 MPa. In about 60 h, the specimen experiences steady-state creep, accelerated creep, and finally failure.

2.5. Testing results of specimen 3

A different schedule was applied to specimen 3 testing (seen in Table 2), which focuses on borehole and rock mass deformation at 500 °C. Figs. 6 and 7 show the axial deformation and borehole radial deformation of specimen 3, respectively. The specimen creeps steadily under 500 °C and 125 MPa hydrostatic pressures. When the hydrostatic pressure increases to 150 MPa, the deformation started to accelerate. With temperature increasing from 500 °C to 600 °C, the specimen shows weakening and softening effect. Apparently accelerated creeping occurs. The radial deformation of borehole and the axial deformation of the specimen show very similar trend.

3. Steady creeping of borehole in granite under high temperature and high pressure

In addition to specimen 2 and 3, steady creep was also observed for specimen 1 when the temperature ranged from 100 °C to 500 °C and hydrostatic pressures were between 12.5 MPa and 125 MPa. The steady-state creep deformation is calculated by removing the immediate elastic deformation and thermal expansion induced by increasing temperature. The steady creep of specimen 1 and 2 at different hydrostatic stresses and temperatures is listed in Tables 3–5.

Table 4
Measured axial creep deformation of specimen 2.

Stress/MPa	Temperature/°C	Single state creep	Creep time/hour	Accumulated creep
25	200	0.29	43.54	0.29
50	200	0.18	43.44	0.47
50	250	0.055	46.36	0.525
75	300	0.13	43.5	0.655
100	400	0.105	26.93	0.76

Table 5
Measured radial creep deformation of specimen 2.

Stress/MPa	Temperature/°C	Measured accumulated creep	Creep time/hour	Adjusted creep deformation
25	200	0.6889	43.54	0.6680
50	200	0.7898	43.44	0.7467
50	250	0.9011	46.36	0.9505
75	300	1.2906	43.5	1.3524
100	400	2.3822	26.93	2.4492
125	500	4.6212	44.56	4.4356

In general, with increasing temperature and hydrostatic pressure, creep deformation is increasing. It is found that the cumulated creep deformation is linearly correlated to temperature and hydrostatic pressure. The relationship is summarized in Table 6. The formula can be used to calculate the anticipated granite creep deformation.

The third equation in Table 6 also presents the relationship between borehole steady-state creep deformation and applied hydrostatic pressure and temperature from testing results of specimen 2. It is found that borehole creep deformation increases exponentially with increasing temperature and hydrostatic stress. In addition, the impact of temperature or hydrostatic pressure is on the same order. Note that the equation only gives the creep deformation at certain temperature and stress. The total borehole deformation should also include elastic deformation and the thermal expansion, which can be expressed in the equation below.

$$U_{\mathrm{rtotal}} = U_{\mathrm{elasticity}} + U_{\mathrm{thermal\ expansion}} + U_{\mathrm{creep}} \tag{1}$$

4. Failure mode and critical condition of borehole in granite

It is observed that when hydrostatic pressure is greater than 125 MPa and the temperature is higher than 500 °C, borehole started collapsing. Granite chips off from the borehole, resulting in borehole diameter increasing. Fig. 8 shows the failure characteristic of specimen at the end of testing. Fig. 9 presents the measured borehole diameter along specimen axis after testing. The followings are also indicated from the deformation data presented in Figs. 4–7.

Borehole deformation is viscoelastic during steady-state creep stage, as explained in the above section. The rock specimens remained intact in the steady-state creep stage. However, granite started to chip off in the borehole and the specimens approached critical condition when the temperature reached 400 °C–500 °C and hydrostatic pressure reached 125 MPa–150 MPa. Borehole deformation indicates visco-plastic-elastic features. With elapse of time, rock specimens started fracturing, followed by the accelerated creep and collapsing of boreholes.

The temperature and hydrostatic pressure associated with failure or critical condition of each tested specimen are listed in Table 7. The three specimens have the same critical instability temperature and the temperature is 500 °C. The critical hydrostatic pressure for the tested specimens ranges from 125 MPa to 150 MPa. Fig. 10 shows the accelerated creep deformation measured for the specimens in critical condition. In terms of engineering practice, stress of 125 MPa and temperature of 500 °C can be established as the critical condition criteria for borehole instability in granite.

Fig. 11 shows the failure mode of specimens after testing. It reveals a cone-shaped failed specimen as well as close to vertical fracture traces on the outside of a specimen. The failure mode is either shearing or combination of shearing and tension.

Table 6
Fitted creep deformation due to thermal and stress.

Creep	Specimen	Strain/displacement	Correlation coefficient
Axial creep deformation/mm	1	$\varepsilon_{zc} = -0.47422 + 0.000773\sigma + 0.003771T$	0.9186
Axial creep deformation/mm	2	$\varepsilon_{zc} = -0.07761 + 0.003346\sigma + 0.000719T$	0.9977
Borehole radial creep deformation/mm	3	$U_{rc} = 0.22767\exp\,(0.004454\sigma + 0.00483T)$	0.9988

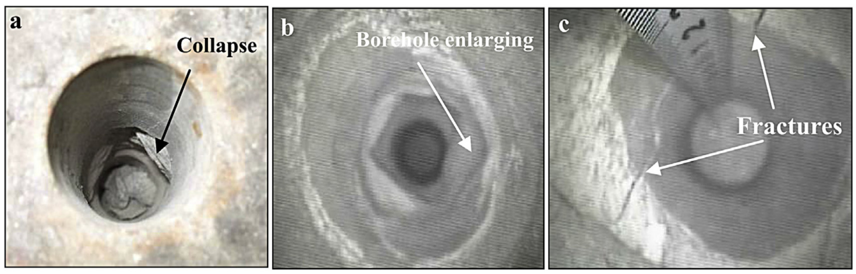

Fig. 8. Granite borehole deformation failure patterns a) Collapse observed by camera; b) Enlarging observed by borescope; c) Fractures in borehole observed by borescope.

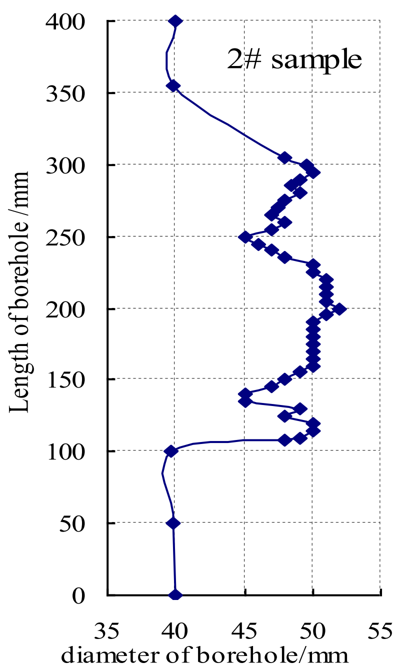

Fig. 9. Variation of borehole diameter along axis (vertical to sample end) after the experiment.

Granite is strong and brittle in room temperature. When borehole in granite failed under high temperature and high stress, borehole walls were observed fracturing and chipping, which contributes to the final collapsing of the hole. It is different from borehole deformation in ductile rocks, which borehole necking is more observed than collapsing.

End effect is also observed during testing due to friction between the specimens and the pressers. The effect may have impacts over about 100 mm long from the specimen ends, which is roughly a quarter of the specimen height. As shown in Fig. 9, the measured borehole diameter increases in the portion of 109 mm up from bottom and 95 mm down from top of specimen 2. The seriously failed portion locates at the middle of the specimen, from 190 mm to 300 mm along the borehole axis. The maximum borehole diameter measured after failure is 52 mm.

According to the maximum strain criterion, the radial critical deformation ratio is measured to be 20%. Using this value in the third equation listed in Table 6,

$$U_{rc} = 0.22767\exp\,(0.004454\sigma + 0.00483T) \tag{2}$$

The critical instability condition criterion for borehole in granite can also be expressed as:

$$\sigma = -1.08442T + 643.5 \tag{3}$$

This equation is illustrated in Fig. 12, which shows the radial critical condition criterion as a function of stress and temperature. Equation (3) also indicates the ultimate rock mass condition for deep drilling. It shows that the drilling may extend deeper when thermal gradient is low. As an example, Kola SG-3 was deepened to 12,262 m. The low thermal gradient at the boring location played a great role.

5. Discussion

The hot dry rock geothermal energy reservoir is high temperature rock mass initially formed from cooling of 650 °C rock or

Table 7
Failure characteristics and critical condition of tested granite specimens.

Specimen	Failure mode	Hydrostatic pressure/MPa	Temperature/°C	Description of failure form
1	Compression and shear failure	150	500	Necking along the hole from 200 to 310 mm. The necking portion is about 100–110 mm in length and 31.5 mm in diameter.
2	Compression shear and tension composite failure	125	500	The middle portion of the hole ruptured and finally collapsed, resulted hole enlargement.
3	Compression shear and tension composite failure	150	500	Apparent fracturing and shear planes along the middle 200 mm of the hole.

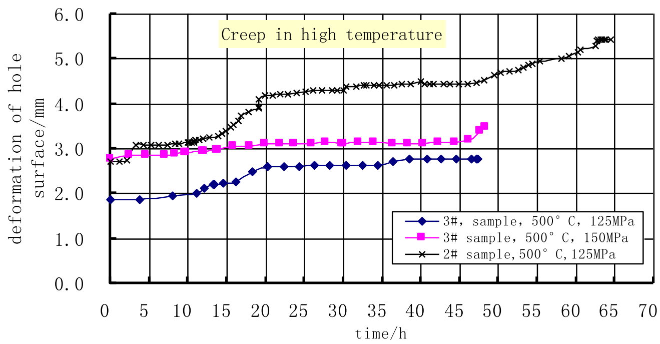

Fig. 10. Creep deformation of borehole with hydrostatic stress 125–150 MPa and temperature 400 °C–500 °C.

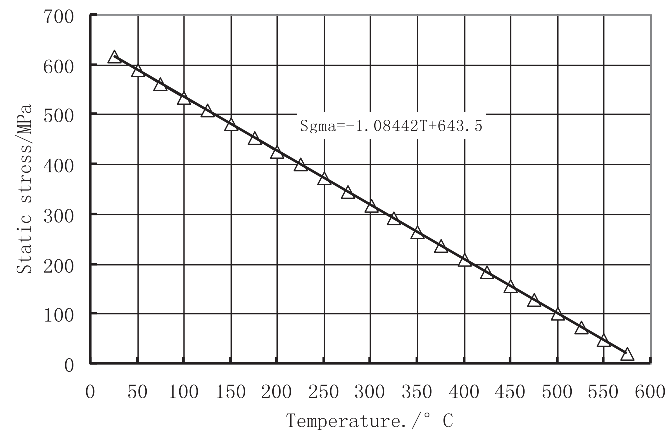

Fig. 12. Critical condition of borehole instability destroy.

higher than 650 °C lava. The mechanical properties of the cooling rock also vary with depth. The stress pattern in rock will change with cooling temperature and pressure. Hence, the ideal rock sample used in the experimental drilling research on HDR geothermal energy extraction is the in-situ one mentioned above. Whereas, it is difficult to conduct laboratory tests on the in-situ rock sample. Coring samples from deep drilling is a direct method which can attain the samples under in-situ geologic condition. However, the rock samples are cooled down by drilling mud circulation and the stress pattern in rock also changes.

While a hole is drilled in hot granite, the wellbore is significantly cooled. Thermal cracking induced by immediately sudden reduction in temperature (i.e. thermal shock) around wellbore will occur while slurry is utilized to cool the drill bit. In the author's previous study, thermal shock can weaken the mechanical and physical properties of granite (such as decrease in elastic modulus, uniaxial compressive strength and tensile strength) more dramatically than thermal cracking induced by slow temperature variation [20]. It is complex to consider the cooling effect on sample. To eliminate cooling effect, the borehole in the granite sample is predrilled at room temperature.

The stress concentration will take place around borehole while a hole is drilled in an established stress medium. Stress concentration is caused by geometric discontinuities involving cracks, sharp corners, holes, and changes in the cross-sectional area of object. Therefore, the stress pattern of borehole here is theoretically same as that around actual wellbore.

Therefore, in order to conduct a feasible and similar lab simulation of deep drilling in granite at high temperature and high pressure, the only way is to employ the cooled rock to heat. Comparing to in-situ rock mass, the rock sample used in lab simulation of deep drilling experiences two processes: cooling from high temperature at in-situ stress state and heating up to high temperature at high experimental stress. These two processes will weaken the rock mechanical properties (i.e. strength, elastic

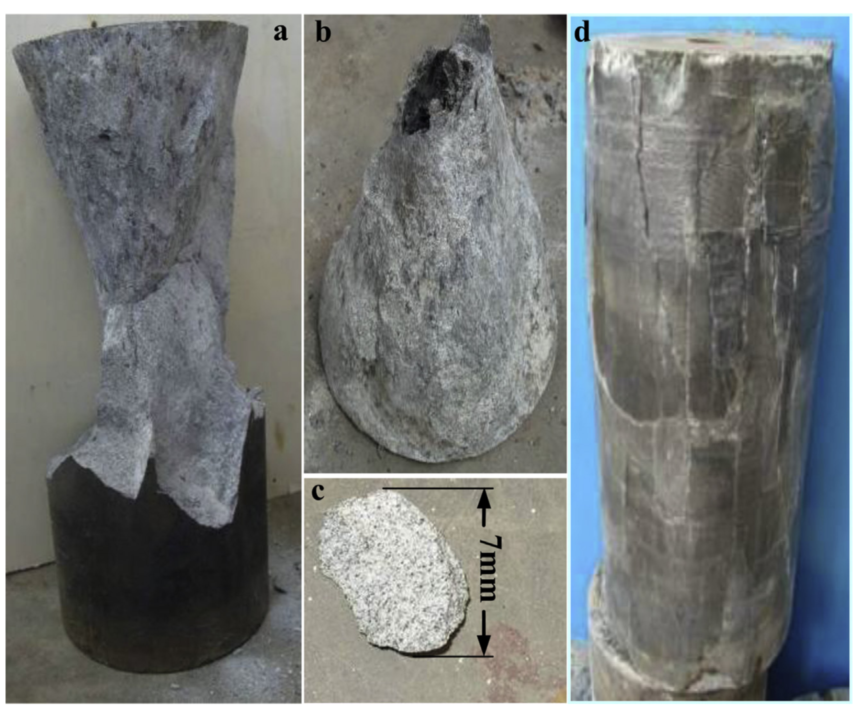

Fig. 11. Compression shear and tensile destruction features photos of the samples 1 and 3 a)shearing failure of sample 1; b) cone from the top of picture a; c) small piece falling down from the damage borehole wall; d) Compression shearing and tension failure mode of sample 3.

modulus et al.). So the borehole will more unstable in the experiment than that in the actual drilling practice at the same temperature and pressure without considering cooling effect during drilling. If the results presented above are applied to drilling engineering practice, the drilling engineering will be safe and successful.

6. Conclusions

This paper presents the testing results of three granite specimens of 200 mm in diameter and 400 mm long using a high temperature and high pressure servo-controlled rock triaxial testing machine. The main conclusions are:

1) In general, borehole deformation increases with increase of stress and temperature. When the hydrostatic pressure is lower than 100 MPa (77% of UCS) and the temperature is below 400 °C, the rock specimen deforms viscoelastically and the borehole is in the steady-state creep stage. The specimen remains intact in this stage. Borehole approaches critical condition when the temperature is between 400 °C and 500 °C and the hydrostatic pressure is 125 MPa (96% of UCS). When temperature reaches 500 °C and the hydrostatic pressure reaches 150 MPa, borehole deformation accelerates sharply and it is followed by failure and collapsing.
2) Radial instability critical condition for borehole in granite is found to be at hydrostatic stress of 150 MPa (115% of UCS) and temperature of 500 °C.
3) The axial deformation increases linearly with the increase of stress and temperature.
4) The radial deformation of borehole in granite increases exponentially with the increase of stress and temperature.
5) The ultimate condition of drilling in granite, in regards to temperature and in-situ stresses, is analyzed based on the maximum strain criterion.

References

[1] Matsunaga Isca. Recent progress of hot dry rock geothermal energy development projects in Japan. Geotherm Resour Counc Bull 1995;24(2):62–4.
[2] Saito Seiji. Recent geothermal well drilling technologies in Kakkonda and Matsukaw, Japan. Geotherm Resour Counc Bull 1991;20(6):166–75.
[3] Baria R, Boumgärtner J, Gérard A. Statue of the European hot dry rock geothermal program. Geotherm Technol 1994;19(1–2):33–48.
[4] Smithson SB, Wenzel F, Ganchin YV, Morozov B. Seismic results at Kola and KTB deep scientific boreholes: velocities, reflections, fluids, and crustal composition. Tectonophysics 2000;329(1–4):301–17.
[5] Haimson BC, Chang C. True triaxial strength of the KTB amphibolite under borehole wall conditions and its use to estimate the maximum horizontal in situ stress. J Geophys Res 2002;107(B10). ETG 15-1–ETG 15-14.
[6] Zhang JC, Xie WW. Status of scientific drilling technology for ultra deep well. Acta Geol Sin 2010;84(6):887–94.
[7] Parker RH. Hot dry rock: geothermal energy: phase 2B final report of the Camborne School of mines project. , New York: Oxford: Pergamon Press; 1989.
[8] Brown DW, Duchane DV. Scientific progress on the Fenton Hill HDR project since 1983. Geothermics 1999;28(4–5):591–601.
[9] Haimson BC. Micromechanisms of borehole instability leading to breakouts in rocks. Int J Rock Mech Min Sci 2007;44(2):157–73.
[10] Lin MZ. Thermal physics of rock and its application. Chongqing: Chongqing University Press; 1991.
[11] David C, Menendez B, Darot M. Influence of stress-induced and thermal cracking on physical properties and microstructure of La Peyratte granite. Int J Rock Mech Min Sci 1999;36(4):433–48.
[12] Heuze FE. High-temperature mechanical, physical and thermal properties of granitic rocks-a review. Int J Rock Mech Min Sci Geomech Abstr 1983;20(1): 3–10.
[13] Boukharov GN, Chanda MW, Boukharov NG. The three processes of brittle crystalline rock creep. Int J Rock Mech Min Sci 1995;32(4):325–35.
[14] Cornet FH, Berard T, Bourouis S. How close to failure is granite rock mass at 5 km depth. Int J Rock Mech Min Sci 2007;44(1):47–66.
[15] Tester JW, Herzog HJ. Economic predictions for heat mining: a review and analysis of hot dry rock (HDR) geothermal energy technology. Energy Laboratory, Massachusetts Institute of Technology; 1990.
[16] Armstead HCH, Tester JW. Heat mining: a new source of energy. London: Chapman & Hall; 1987.
[17] Hirofumi M, Toshihiro U, Masakatsu S. Deep geothermal resources survey program: igneous, metamorphic and hydrothermal processes in a wall encountering 500 °C at 3729 m depth, Kakkonda, Japan. Geothermics 1998;27(5–6):507–34.
[18] Zhao YS, Wan ZJ, Feng ZJ, Yang D, Zhang Y, Qu F. Triaxial compression system for rock testing under high temperature and high pressure. Int J Rock Mech Min Sci 2012;52:132–8.
[19] Jaeger JC, Cook NGW. Fundamentals of rock mechanics. 3rd ed. London: Chapman and Hall; 1979.
[20] Xi BP, Zhao YS. Experimental research on mechanical properties of water-cooled granite under high temperatures within 600 °C. Chin J Rock Mech Eng 2010;29(5):0892–8.